

Study of the Effect of Gas Channels Geometry on the Performance of Polymer Electrolyte Membrane Fuel Cell

62(1), pp. 97-105, 2018

<https://doi.org/10.3311/PPch.9369>

Creative Commons Attribution

Nima Ahmadi^{1*}, Sajad Rezazadeh¹, Abdolrahman Dadvand¹,
Iraj Mirzaee¹

RESEARCH ARTICLE

Received 24 April 2016; accepted after revision 17 August 2016

Abstract

This study focuses on the effect of gas channels geometry on the performance of polymer electrolyte membrane fuel cell. A set of empirical tests are accomplished to study these effects. The cross section of the gas channel is changed from square to inverse trapezoid, that is, the bottom width of the channel is kept fixed at 1mm while the width of the top of the channel is increased with the discontinuity of 0.2mm from 1mm to 1.6mm. Results show that the best performance is obtained for the inverse trapezoid channel with the 1.2mm width in the top section of channel. Moreover to verify the experimental test results, a 3-D finite volume method in-house code is brought up to solve the conservation equations. Hereafter, the nozzle shape gas channel efficacy is investigated experimentally and the obtained results are verified by numerical results. The obtained results determine that, at an equable voltage, this new configuration of the channels enhances the current density output by cells as compared to the primary model (i.e., gas channel with square cross section area). This finding may be due to the increase of reactant velocity in the channel.

Keywords

Channel geometry, Polymer Electrolyte Membrane Fuel Cell, Nozzle shape channel, Finite volume

1 Introduction

PEMFC (Polymer Electrolyte Membrane Fuel Cell), which exerts an extenuate polymer membrane as electrolyte has been considered as an applicant of comer energy resources, exclusively for traffic utilization and habitable power. The PEMFC has significant advantages such as major proficiency, clarity, silence, slight operating temperature, capability of prompt launching, no liquid electrolyte and simple cell design. However, before this system becomes competitive with the traditional combustion power plants its performance and cost should be further optimized [1-3].

Recently, researches about fuel cells and fuel cell systems have been progressed. However, their cost is still too high to become feasible commercial products.

In a fuel cell, fuel as hydrogen together with an Oxidizing like oxygen breed power and heat and water are typical products of the fuel cell operation. The working principle of a typical fuel cell can be described as follows: as the hydrogen gas flows into the fuel cell on the anode side a platinum catalyst facilitates oxidation of the hydrogen gas producing electrons (e^-) and hydrogen ions (H^+). Hydrogen ions transfer among the membrane (the centre of the fuel cell separating the anode and the cathode) and then combine with oxygen and electrons on the cathode side with the aid of a catalyst layer made from platinum to produce water. The electrons, which are unable to pass through the membrane, transmit from the anode to the cathode via an external electrical circuit.

The anode and the cathode are both porous and made from a material which conducts electricity, as usual carbon. Electrode external faces are in contact with the membrane, which contains carbon, polymer electrolyte and a platinum-based catalyst. The oxidation and reduction fuel cell half reactions happen respectively in the anode and cathode cracking pads. The reactant gases are penetrated via porous electrodes. These electrodes are generally designed for maximum surface area per unit material volume. Accordingly, gas diffusion layer (GDL) would be attainable for the reactions in order to minimize the transport resistance of the hydrogen and oxygen in active layers.

In the past decade, extensive researches have been conducted to develop realistic simulation models for fuel cell systems. The attempts are mainly focused on the optimization of

¹Mechanical Engineering School, Urmia University of Technology, Urmia, Iran

*Corresponding author, e-mail: nima.ahmadi.eng@gmail.com

fuel cell systems to make them cost competitive with currently available energy conversion devices [4].

A number of studies have examined various aspects of PEM fuel cell performance as a function of operating conditions (see [5–13] for examples) in order to find ways to improve its performance. One significant tool in the optimization study of fuel cell performance is computational modelling, which can help understand the fundamental phenomena taking place in the fuel cell system [14].

The performance of a PEM fuel cell is influenced by many factors including operating temperature, pressure, the gas flow moisture and the geometrical parameters. Among the various aspects of that affect PEMFC's proficiency, geometrical formations have a considerable obligation. Proverbially, it is known that the performance of a fuel cell with smaller shoulder widths is better than those with larger ones [15–18].

Effect of gas channel geometry on the performance of PEM fuel cells was studied by Majidifar et al. [19] via bringing up new shape, such as trapezoidal inlet shape for gas channel. Ahmadi et al. [20] handled PEMFC performance in various voltages [20]. Ahmadi et al. [21] considered impression of parallelogram gas channel and shoulder geometry on the PEM fuel cell proficiency [21]. Ahmadi et al. [22] scrutiny the effect of prominent gas-diffusion layers on the PEM fuel cell efficiency [22]. Ahmed and Sung implemented studies for PEM fuel cells with a new design for the channel shoulder geometry [23].

In the present work, the effect of increasing the width of the gas channel at the upper region, on the fuel cell performance, is investigated. For this reason the channel width in the upper section is increasing from 1mm to 1.2mm, then 1.4mm and finally to 1.6mm via maintaining the width of the underneath segment equal to 1mm. henceforth the nozzle shape reactant gas channel efficacy is studied on the fuel cell performance and velocity distribution.

2 Mathematical modelling

The model considered in the present work is a single straightway gas channel, 3-D PEMFC system. The current system enfolds gas flow channels, current collector plates, GDLs, catalyst layers, and an electrolyte membrane. Figure 1 shows the schematic of a single cell of a PEM fuel cell.

2.1 Assumptions

The following assumptions were made in order to develop the mathematical model: the gas mixture is considered as ideal gas and due to low speed of flow, it is assumed to be laminar, steady-state, incompressible. The Membrane Electrode Assembly (MEA) which is composed of membrane, GDLs and catalyst layers, is isotropic, as long as the layers contact resistance is imperceptible. The liquid velocity inside the flow channels is almost equal to the gas velocity. Thermal conductivity coefficient for components is fixed. It is noteworthy that the electrodes

are electrically insulated, the membrane is considered impenetrable for reactant gases and the leakage current is null.

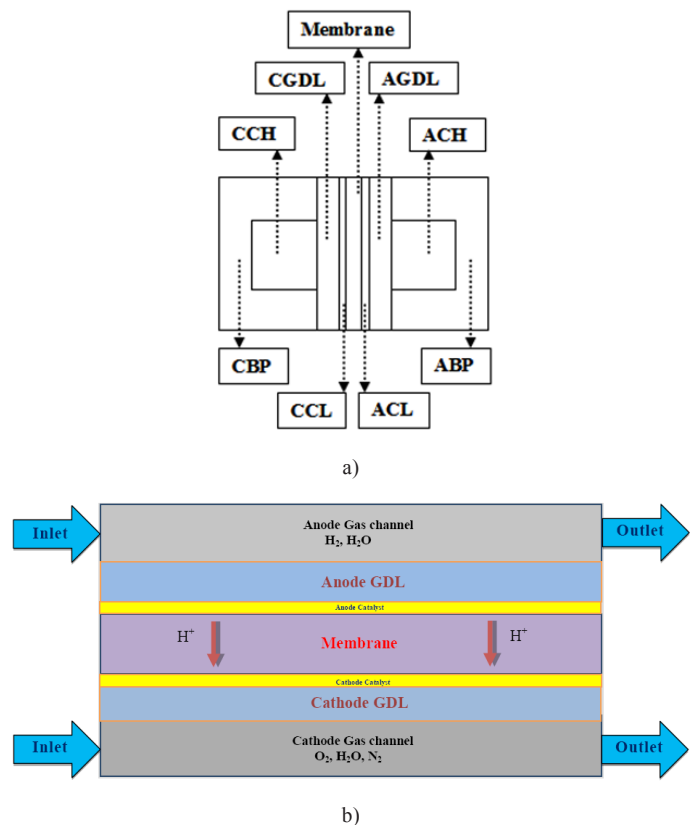


Fig. 1 Schematic of a single cell of a conventional (base case) PEM fuel cell a); Side view of the base case b)

2.2 Governing equations

In the fuel cell varied layers transport Phenomenon is modelled using mass, momentum, species, charge and energy conservation equations.

Mass conservation equation:

$$\nabla \cdot \rho \vec{u} = 0 \quad (1)$$

Where ρ is the density of gas mixture and \vec{u} is the velocity vector in fluid is defined as: Mass source terms are omitted due to the assumptions made in Section 2.1.

Momentum conservation equations:

$$\frac{1}{(\epsilon^{eff})^2} \nabla \cdot (\rho \vec{u} \vec{u}) = -\nabla P + \nabla \cdot (\mu \nabla \vec{u}) + S_u \quad (2)$$

In the last equation ϵ^{eff} interprets the drastic porosity entrant the porous mediums and μ is the viscosity of the gas mixture. S_u is the source term that is used to represent Darcy's drag for flow through porous gas diffusion layers and catalyst layers and is defined as:

$$S_u = \frac{\mu}{\beta} \vec{u} \quad (3)$$

Due to last Eq., permeability in porous mediums is indicated by β .

Species conservation equation:

$$\nabla \cdot (\vec{u}C_k) = \nabla \cdot (D_k^{eff} \nabla C_k) + S_k \quad (4)$$

In Eq. (4), the subscript k represents the chemical species including hydrogen, water in anode side and oxygen, nitrogen and water in cathode side. D_k^{eff} marks the impressive diffusion factor that is defined to describe the porosity effects in the porous gas diffusion and catalyst layers of species via the Bruggeman relevance [24, 25]:

$$D_k^{eff} = (\varepsilon^{eff})^{1.5} D_k \quad (5)$$

Here, D_k is the diffusion coefficient, which is a function of temperature and pressure [25],

$$D_k = D_k^0 \left(\frac{T}{T_0} \right)^{3/2} \left(\frac{P_0}{P} \right) \quad (6)$$

In addition, the source terms associated with species are defined as [25]:

$$S_k = \begin{cases} 0 & \text{Flow channels} \\ 0 & \text{GDL} \\ -\nabla \cdot \left(\frac{n_d}{F} I \right) - \frac{S_k J}{nF} & \text{Catalyst layers} \\ -\nabla \cdot \left(\frac{n_d}{F} I \right) & \text{Membrane} \\ 0 & \text{Bipolar plates} \end{cases} \quad (7)$$

Charge conservation equation [25]:

$$\nabla \cdot (\sigma_e^{eff} \nabla \varphi_e) + S_\varphi = 0 \quad (8)$$

In Eq. (8), σ_e and φ_e are the ionic conductivity in the membrane, and the electrolyte phase potential, respectively. The source term S_φ in the catalyst layers describes the current density transfer. In the other sub-layers no source term is needed. The ionic conductivity in the membrane σ_e is defined as [25]:

$$\sigma_e = \left(0.514 \frac{M_{m,dry}}{\rho_{m,dry}} C_w - 0.326 \right) e^{1268 \left(\frac{1}{303} - \frac{1}{T} \right)} \quad (9)$$

Where C_w is the water vapour concentration defined as [25]:

$$C_w = \frac{\rho_{m,dry}}{M_{m,dry}} \lambda \quad (10)$$

Where $\rho_{m,dry}$ and $M_{m,dry}$ are the material density and the equivalent weight of a dry PEM, respectively. In addition, λ denotes the water content in the catalyst layer [25].

$$\sigma_e^{eff} = \varepsilon_m^{1.5} \sigma_e \quad (11)$$

Where, ε_m denotes the volume fraction of the membrane phase in the catalyst layer. The number of water molecules, which are transmitted by each sulfonate (Sulfonate is a sulfonic acid. In other word it contains $-SO_3^-$ group) group in the membrane determines the water content [25]:

$$\lambda = \begin{cases} 0.043 + 17.18a - 39.85a^2 + 36a^3 & (a < 1) \\ 14 + 1.4(a - 1), & (a > 1) \end{cases} \quad (12)$$

Here, a is the water activity and is defined as [25]:

$$a = \frac{P_{wv}}{P_{Sat}} \quad (13)$$

Where

$$P_{wv} = x_{H_2O} P \quad (14)$$

Here, P_{wv} is water vapour pressure and saturation pressure and x_{H_2O} denotes the mole fraction of water.

The energy equation is given as [25]:

$$\nabla \cdot (\rho \vec{u} T) = \nabla \cdot (\lambda_{eff} \nabla T) + S_T \quad (15)$$

Where λ_{eff} denotes the effective thermal conductivity and S_T is the source term, which is defined through the following equation:

$$S_T = I^2 R_{ohm} + h_{reaction} + \eta_{an} i_{an} + \eta_{ca} i_c \quad (16)$$

In Eq. (17), $h_{reaction}$ represents the heat produced via the chemical reactions and R_{ohm} is the membrane ohmic resistance, which is defined as,

$$R_{ohm} = \frac{t_m}{\sigma_e} \quad (17)$$

Where, in the last expression membrane stoutness is shown via t_m . η_a and η_c are the over potentials of anode and cathode respectively and they are calculated using the following expressions [25]:

$$\eta_a = \frac{RT}{\alpha_a F} \ln \left[\frac{IP}{j_{0a} P_{O_2}} \right] \quad (18)$$

$$\eta_c = \frac{RT}{\alpha_c F} \ln \left[\frac{IP}{j_{0c} P_{H_2}} \right] \quad (19)$$

In Eq. (19) and (20) α_a and α_c are the anode and cathode transfer factor. Partial pressure of hydrogen and oxygen is offered with P_{O_2} . j_0 is the reference exchange current density. Moreover, I is the residential current density of the cell, which is defined as [25]:

$$I = \frac{\sigma_e}{t_m} \{ V_{OC} - V_{Cell} - \eta \} \quad (20)$$

Where V_{OC} is the open circuit voltage and η represents the losses. Equation (21) can be rewritten as:

$$V_{Cell} = V_{OC} - \eta - \frac{t_m}{\sigma_e} I \quad (21)$$

The fuel and oxidant fuel rate \mathbf{u} is given by following equations [25]:

$$\mathbf{u}_{in,a} = \frac{\xi_a I_{ref} A_m}{2C_{H_2,in} F A_{ch}} \quad (22)$$

$$\mathbf{u}_{in,c} = \frac{\xi_c I_{ref} A_m}{4C_{O_2,in} F A_{ch}} \quad (23)$$

Where, I_{ref} and ξ are respectively the reference current density and stoichiometric ratio (i.e., the ratio of the amount of fuel supplied to that required based on the reference current density). The species concentrations of the flow inlets are assigned by the humidification conditions of both the anode and cathode inlets.

2.3 Boundary conditions

Boundary conditions are applied as follows. A constant mass flow rate and constant pressure are applied respectively at the channel inlet and channel outlet. The no-flux conditions are employed for mass, momentum, species and potential conservation equations at all boundaries except for the inlet and outlet boundaries of the anode and cathode flow channels.

3 Experimental tests and numerical procedure

In the present work, experimental and numerical analyses were performed to investigate the effect of geometrical configuration of the gas channel on the performance of PEM fuel cell. Figure.2 depicts the schematic of the experimental set up. The geometrical parameters and operating conditions related to the base case, which are identical to those used in [24], are given in Tables 1 and 2, respectively. A multiphase model was developed to numerically simulate the fuel cell behaviour. A home-generated code based on the finite volume technique was developed to solve the governing equations. After grid independence test, a structured grid with 166325 cells was chosen for all the simulations carried out in the present work.

Table 1 Configuration and operating qualification [24]

Parameter	Value
Gas channel length	5.0×10^{-2} m
Gas channel width and depth	1.0×10^{-3} m
Bipolar plate width	5.0×10^{-4} m
Gas diffusion layer thickness	3.0×10^{-4} m
Catalyst layer thickness	1.29×10^{-5} m
Membrane thickness	1.08×10^{-4} m
Cell temperature	343K
Anode pressure	3 atm
Cathode pressure	3 atm
Anode and cathode humidity	100%

Table 2 Operating conditions of PEM fuel cell [24]

Parameter	Symbol	Value
Electrode porosity	E	0.4
Electrode conductivity (S/m)	σ_e	100
Membrane ionic conductivity (S/m)	σ_m	17.1223
Transfer coefficient, anode side	α_a	0.5
Transfer coefficient, cathode side	α_c	1
Cathode Ref. exchange current density (A/m ²)	$i_{o,c}^{ref}$	1.8081e-3
Anode Ref. exchange current density (A/m ²)	$i_{o,a}^{ref}$	2465.598
Electrode thermal conductivity (W/m.K)	k_{eff}	1.3
Thermal conductivity of membrane (W/m.K)	K_{mem}	0.455
Electrode hydraulic permeability (m ²)	K_p	1.76e-11

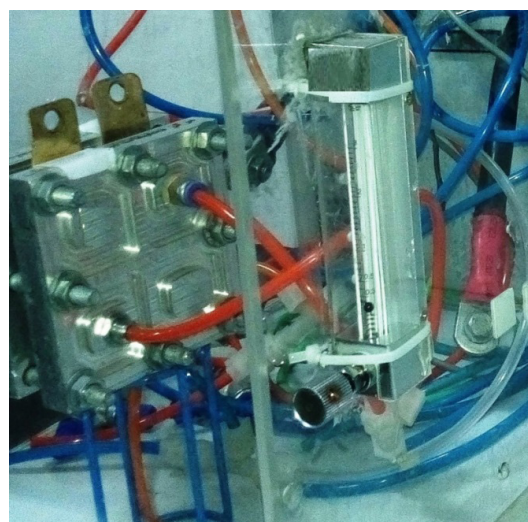


Fig. 2 Schematic of PEM fuel cell experimental set-up

4 Results and Discussion

4.1 Validation of the current numerical and experimental results

In numerical model the structured meshes are used. At the catalyst layers where the electro chemical reactions occur, the meshes are finer. Also a grid independence test was implemented and finally the optimum number of elements (174 000) chosen. The quality of all meshes due to Equi-Size skew method is less than 0.1. Figure 3a shows grid independence test. The number of iterations is determined as 2000 for low current density and 12000 for high current density. An IBM-PC-quad core (CPU speed is 2.4 GHz) was used to solve the set of equations. The computational time for solving the set of equations was 7 h. In order to substantiate the accuracy of the current numerical results, the polarization and power density curves associated with the base model are compared with our experimental results and the experimental results found by Wang et al. [24] (see Fig. 3b). The geometrical parameters

and operating conditions related to this base case are given in Tables 1 and 2. As it is observed, Fig. 3 reveals a good agreement between the current numerical and experimental results and the experimental results Achieved from Wang et al. study results [24].

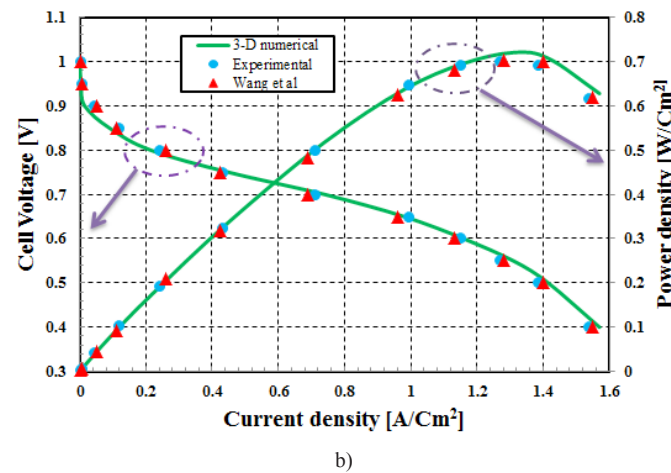
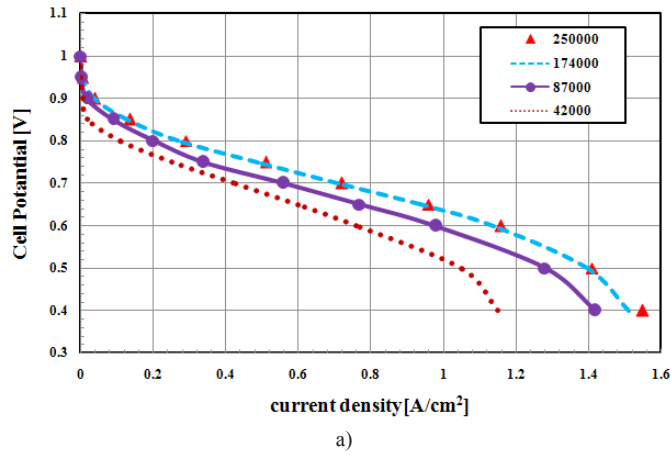


Fig. 3 a) grid independence test; b) Polarization and power density curve; comparison between the current numerical and experimental results and the experimental results of [24].

4.2 Effect of gas channels inlet shape

In this section, the influence of the channels inlet shape and size on the performance of the fuel cell is investigated. For this reason, we conducted experimental and numerical tests for four different cases shown in Fig. 4 to study the effects of configuration of the gas channel cross section on the performance of the cell. It may be noted that the Case 1 is identical to the base case for which the cross section of the gas channels is square. In the other three cases, the cross section of the gas channel has been changed to an inverse trapezoidal shape, where the area of shoulder of bipolar plates and cell (bottom) width are still kept fixed. These cases are distinguished by different sizes of the top width of the gas channel. Four different sizes of the top width of the gas channel, namely, 1mm, 1.2mm, 1.4mm and 1.6mm are considered. The results associated with the four cases are compared to investigate the effect of geometrically different gas channel shapes on the current density produced by cell and species distribution.

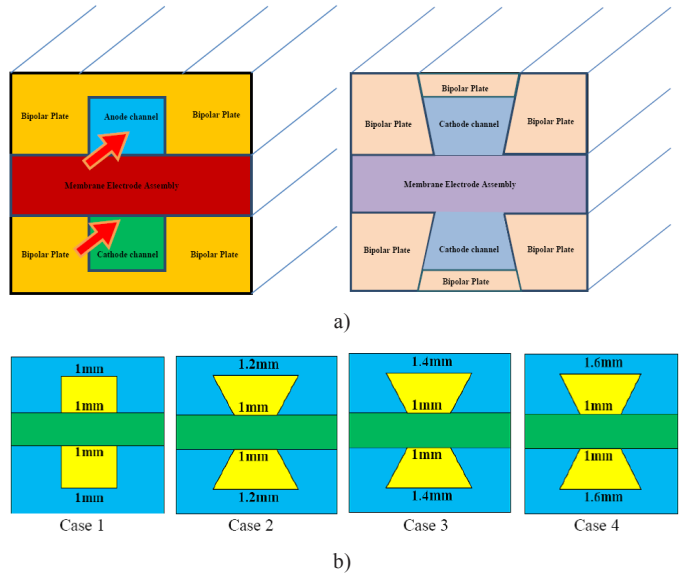


Fig. 4 a) Schematic of different geometrical configurations; b) Front views of different geometrical configurations

Cell voltage versus current density is shown in Fig. 5. It can be seen that at a constant cell voltage the current density for the Case 2 is slightly higher than that of the other cases. This is the case for both the experimental and numerical results. In addition, the ohmic loss in the Case 2 is lower than that of other cases (see Fig. 6). Consequently, the protonic conductivity in the Case 2 is higher than that of the other cases (see Fig. 7). This finding can also be figure out via Eq. (9).

As shown in Fig. 6, the maximum value of ohmic loss is observed in the channel area and it grows in flow direction. This can be attributed to the fact that the main parameter influencing the ohmic loss is the protonic conductivity. The protonic conductivity in shoulder area is more than that in the channel area and it is increased along the PEMFC (presented in Fig. 7). The protonic conductivity revolves by temperature and membrane water content. In addition, the water content depends on water activity. For the different four cases considered in the present work, the water activity distribution at the interface of the cathode catalyst layer and membrane is depicted in Fig. 8. Note that in this figure the cell voltage is considered to be equal to 0.6 V.

Figure 9 indicates the oxygen distribution at the inlet and outlet of the cell. It is observed that Case 2 has consumed more amount of oxygen compared to the other cases revealing its best performance.

5 Effect of Converged nozzle like Gas channel

To study the effect of nozzle like gas channels effects, the width of the channel is diminished once from left and right with a slope of $\phi=0.005^0$ (Case 2) from inlet to outlet and again the test was accomplished with $\phi=0.01^0$ (Case 3) (The case study schematic is shown in Fig. 10). Case 1 has constant shape with no slope (base model and $\phi=0$).

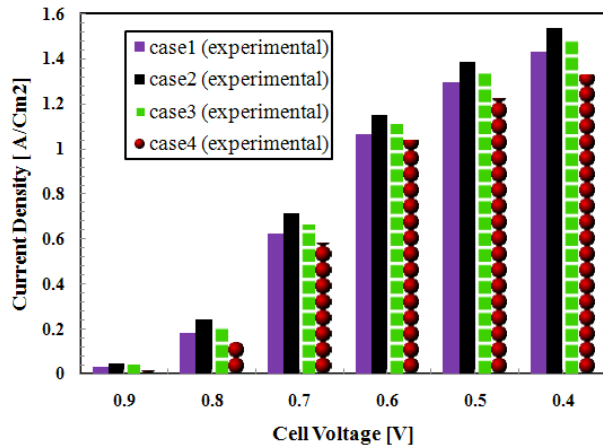
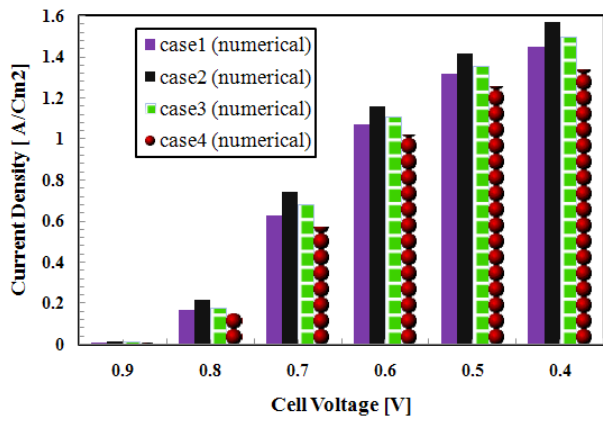


Fig. 5 Polarization diagrams associated with different cases Case 1 (rectangular), Case 2 (1.2mm), Case 3 (1.4mm), Case 4 (1.6mm)

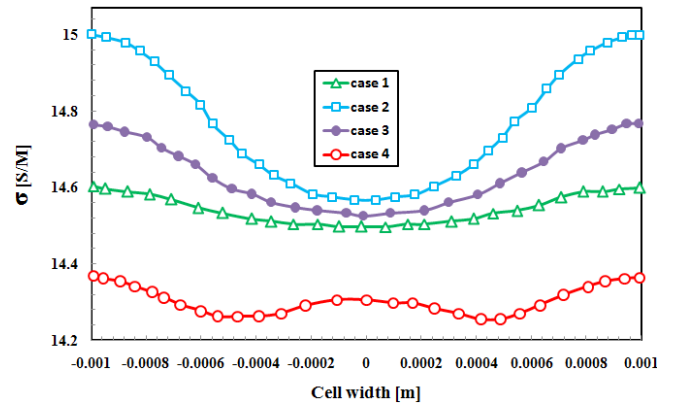
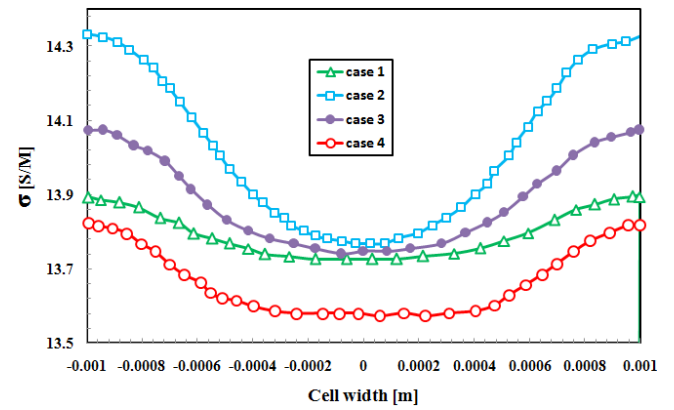


Fig. 7 Comparison of membrane conductivity at the membrane-cathode interface of catalyst attained at 0.6V; (above) entry region, (below) exit region Case 1 (rectangular), Case 2 (1.2mm), Case 3 (1.4mm), Case 4 (1.6mm)

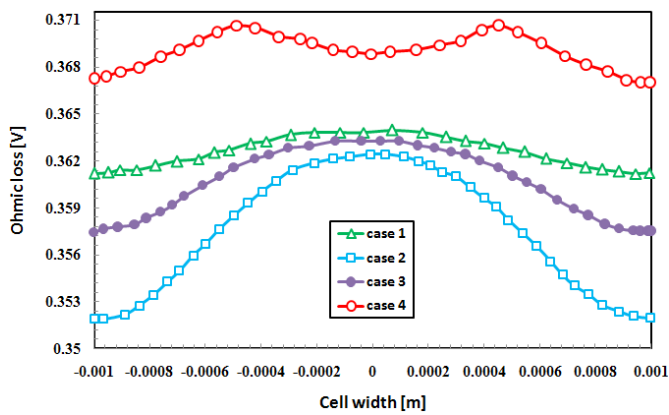
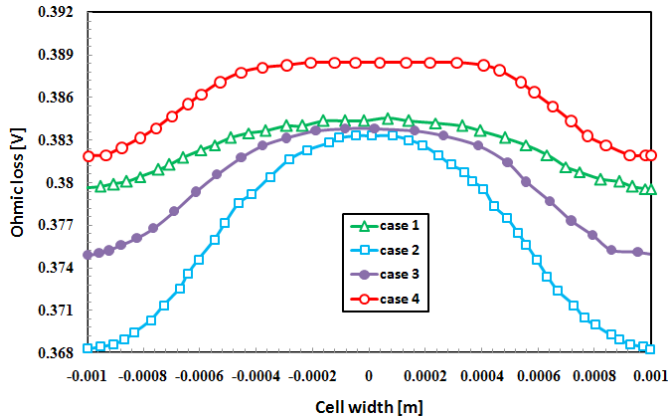


Fig. 6 Comparison of ohmic loss at the membrane-cathode interface of catalyst attained at 0.6V; (above) entry region, (below) exit region. Case 1 (rectangular), Case 2 (1.2mm), Case 3 (1.4mm), Case 4 (1.6mm)

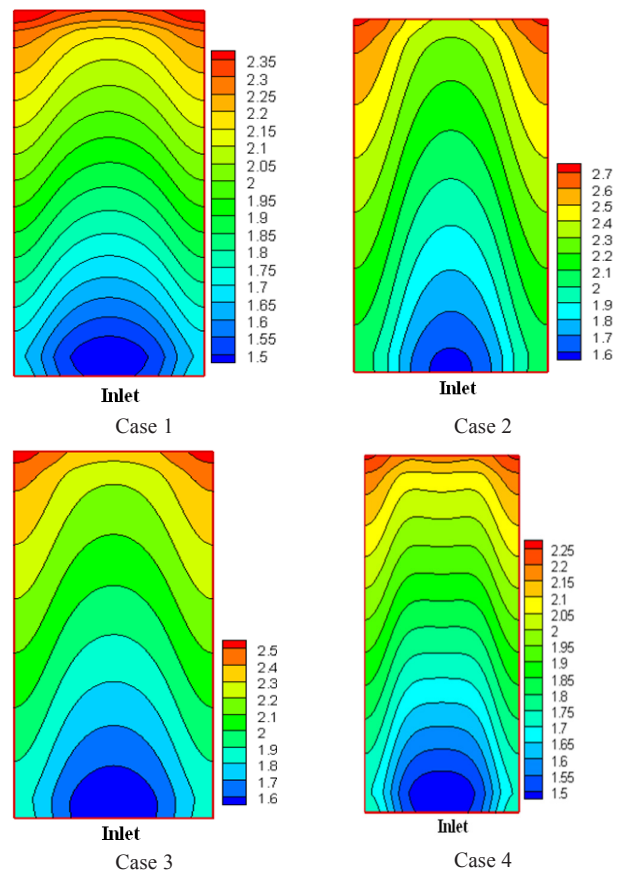


Fig. 8 Comparison of water activity of different cases Case 1 (rectangular), Case 2 (1.2mm), Case 3 (1.4mm), Case 4 (1.6mm)

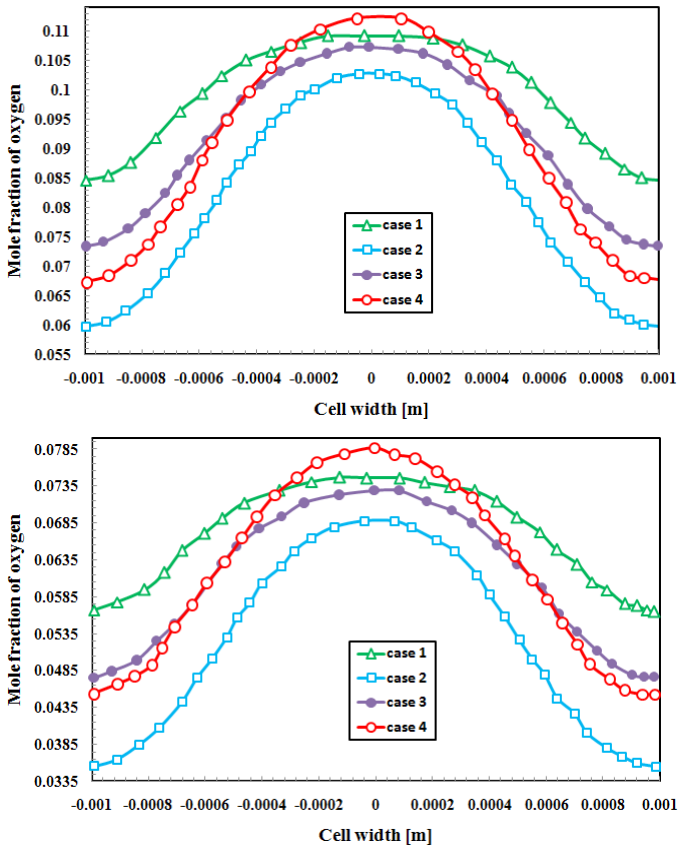


Fig. 9 Comparison of oxygen mole fraction at the catalyst's membrane-cathode interface in 0.6 V; (above) entry region (below) exit region. Case 1 (rectangular), Case 2 (1.2mm), Case 3 (1.4mm), Case 4 (1.6mm)

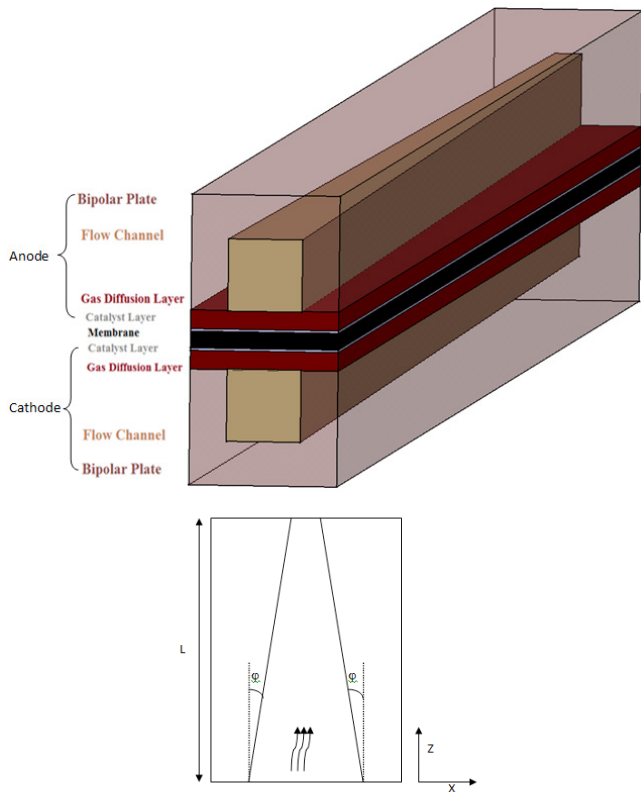


Fig. 10 Nozzle like channel: isometric (above); top view (below)

Figure 11 presents the oxygen molar concentration at the interface of cathode catalyst layer and membrane along the cell for the base model (Case 1) and Cases 2 and 3. Oxygen consumption is the main parameter which affects the cell output current density. It is clear that Case 2 consumes more oxygen magnitude, therefore it is expected the Case 2 produces more current density than other two cases at same voltages. This fact is observed in polarization curve of three different cases in Fig. 12.

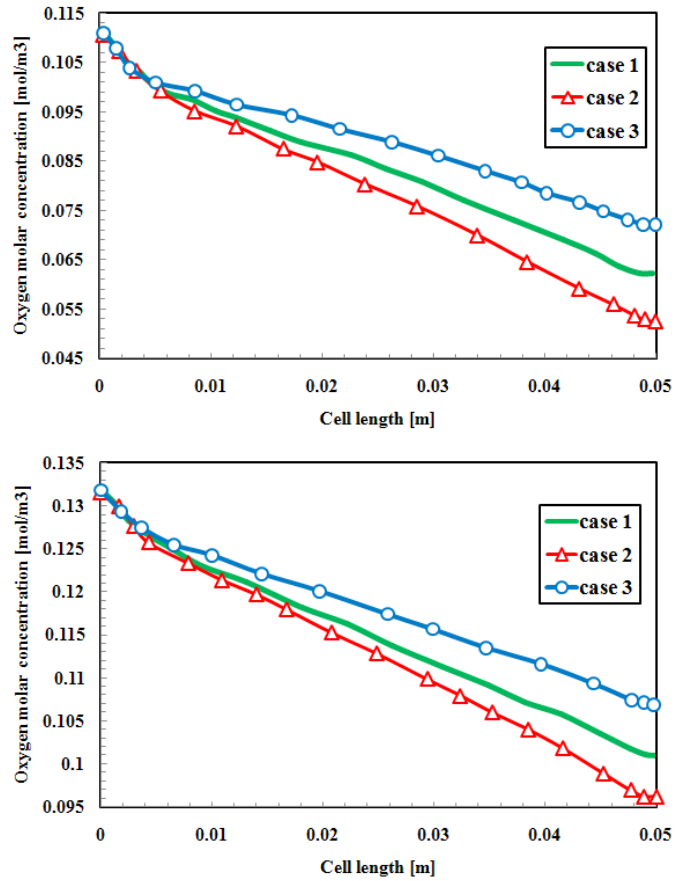


Fig. 11 Comparison of oxygen concentration for three different cases attained at 0.4V: (above) and 0.6V (below) Case 1 (base model), Case 2 ($\phi=0.005^\circ$), Case 3 ($\phi=0.01^\circ$)

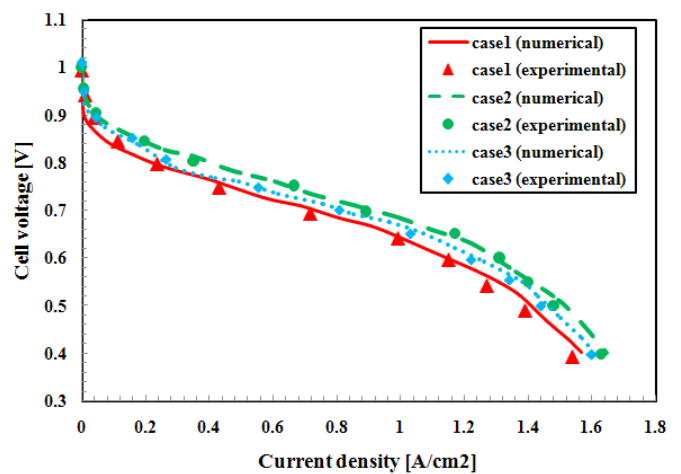


Fig. 12 Polarization curve for three cases Case 1 (base model), Case 2 ($\phi=0.005^\circ$), Case 3 ($\phi=0.01^\circ$)

In Fig. 11 it can be seen that the Case 2 has the minimum value of oxygen concentration along the cell. It is due to excessive consuming of the oxygen along the cell. Nozzle like shapes of channel lead to increasing in reactant gases velocity in the channel without further energy utilizing. Decreasing the inlet area front of the flow leads to increasing the velocity which helps to reactant to reach reaction area better and further monotonous. Also enhancing the velocity magnitude touch the diffusion term of the species conservation also has a major impression on the convection term of mentioned equation. Figure 13 compares the velocity magnitude for three different cases in the middle of the cathode gas channel.

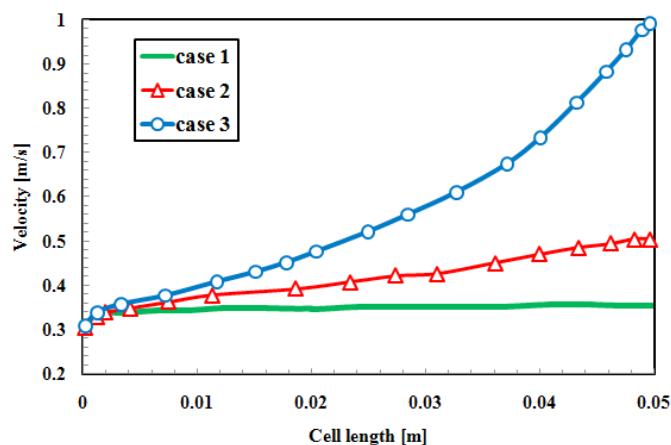


Fig. 13 Comparison of velocity magnitude for three cases Case 1 (base model), Case 2 ($\phi=0.005^\circ$), Case 3 ($\phi=0.01^\circ$)

As can be seen in Fig. 13, Case 2 has maximum velocity magnitude in the cathode side gas channel. This abrupt increment in velocity slightly overcomes the reactant transfer to the reaction areas. In the other word large magnitude of velocity don't give enough time to reactant gas to diffuse to the GDLs. Via considering Fig. 11 it is found that at the exit region of the cell (in Case 3) a large amount of the oxygen have not enough time to diffuse the GDL. But in the general case, nozzles like channels improve the species diffusion and help the reactant to distribute more uniform in the reaction areas.

6 Conclusions

In the present investigation we focused on the improvement of the PEMFC performance by changing the geometrical configuration of the gas channels. For this reason a set of experimental and numerical tests were accomplished to study these effects and verify the results. First in present work the effect of gas channel inlet shape has changed from square to inverse trapezoidal shape. At the following the effect of increasing gas channels width in top section of channel at fixed PEMFC breadth. The breadth of reactant gas channel is growth from 1mm to 1.2mm, 1.4mm and 1.6mm. The results of all cases are compared to each other and it is understood that Case 2 has the best dimension and formation. Thereafter the effects

of the nozzle shape gas channels were studied experimentally and numerically in more details. It can be seen that nozzle like channel has a great effect to increase the PEMFC performance by growing the velocity quantity. To investigate these efficacies, the reactant gas channels width once with a sloop of $\phi=0.01$ degree (Case 3) decremented from inlet to the outlet (at the constant cell width) as Case 3. Again the channel width is reduced with the sloop of $\phi=0.005$ degree (Case 2) in inlet to outlet as Case 2. The experimental and numerical results show that nozzle like channels increase velocity magnitude and helps species to reach easily and more uniform to reaction areas. Also it can be found that Case 2 has the best performance unlike the two other cases.

Nomenclature

Water activity	a
Molar concentration [mol m^{-3}]	C
Mass diffusion coefficient [$\text{m}^2 \text{s}^{-1}$]	D
Faraday constant [C mol^{-1}]	F
Local current density [A m^{-2}]	I
Exchange current density [A m^{-2}]	J
Permeability [m^2]	K
Molecular mass [kg mol^{-1}]	M
Electro-osmotic drag coefficient	n_d
Pressure [Pa]	P
Universal gas constant [$\text{J mol}^{-1} \text{K}^{-1}$]	R
Temperature [K]	T
Thickness	T
Velocity vector	\mathbf{u}
Cell voltage	V_{cel}
Open-circuit voltage	V_{oc}
Width	W
Mole fraction	X
<i>Greek Letter</i>	
Water transfer coefficient	α
Effective porosity	ϵ^{eff}
Density [kg m^{-3}]	ρ
Electrolyte phase potential (varies from -1 to 1) [v]	Φ_e
Viscosity [$\text{kg m}^{-1}\text{s}^{-1}$]	μ
Membrane conductivity [$\text{1.ohm}^{-1}\text{m}^{-1}$]	σ_m
Water content in the membrane	λ
Stoichiometric ratio	ζ
Over potential [v]	η
Effective thermal conductivity [$\text{w m}^{-1}\text{k}^{-1}$]	λ_{eff}
<i>Subscripts and superscripts</i>	
Anode	a
Cathode	c
Channel	ch
Chemical species	k
Membrane	m
Membrane electrolyte assembly	MEA

Reference value	ref
saturated	sat
Water	w

References

- [1] Kilic, M. S., Korkut, S., Hazer, B. "Electrical Energy Generation from a Novel Polypropylene Grafted Polyethylene Glycol Based Enzymatic Fuel Cell." *Analytical Letters*. 47(6), pp. 983–995. 2014. <https://doi.org/10.1080/00032719.2013.860536>
- [2] Karthikeyan, R., Uskaikar, H. P., Berchmans, S. "Electrochemically Prepared Manganese Oxide as a Cathode Material for a Microbial Fuel Cell." *Analytical Letters*. 45(12), pp. 1645–1657. 2012. <https://doi.org/10.1080/00032719.2012.677786>
- [3] Saheb, A. H., Seo, S. S. "Polyaniline/Au Electrodes for Direct Methanol Fuel Cells." *Analytical Letters*. 44(12), pp. 2221–2228. 2011. <https://doi.org/10.1080/00032719.2010.546031>
- [4] Grujicic, M., Chittajallu, K. M. "Design and optimization of polymer electrolyte membrane (PEM) fuel cells." *Applied Surface Science*. 227, pp. 56–72. 2004. <https://doi.org/10.1016/j.apsusc.2003.10.035>
- [5] Xing, X. Q., Lum, K. W., Poh, H. J., Wu, Y. L. "Optimization of assembly clamping pressure on performance of proton-exchange membrane fuel cells." *Journal of Power Sources*. 195(1), pp. 62–68. 2010. <https://doi.org/10.1016/j.jpowsour.2009.06.107>
- [6] Chang, W. R., Hwang, J.-J., Weng, F.-B., Chan, S.-H. "Effect of clamping pressure on the performance on a PEM fuel cell." *Journal of Power Sources*. 166, pp. 149–154. 2007. <https://doi.org/10.1016/j.jpowsour.2007.01.015>
- [7] Lange, K. J., Sui, P.-C., Djilali, N. "Determination of effective transport properties in a PEMFC catalyst layer using different reconstruction algorithms." *Journal of Power Sources*. 208, pp. 354–365. 2012. <https://doi.org/10.1016/j.jpowsour.2011.11.001>
- [8] Amphlett, J. C., Baumert, R. M., Mann, R. F., Peppley, B. A., Roberge, P. R., Harris, T. J. "Performance modeling of the Ballard Mark IV solid polymer electrolyte fuel cell. I. Mechanistic model development." *Journal of The Electrochemical Society*. 142, pp. 9–15. 1995. <https://doi.org/10.1149/1.2043866>
- [9] He, G., Yamazaki, Y., Abudula, A. "A three-dimensional analysis of the effect of anisotropic gas diffusion layer(GDL) thermal conductivity on the heat transfer and two-phase behavior in a proton exchange membrane fuel cell(PEMFC)." *Journal of Power Sources*. 195, pp. 1551–1560. 2010. <https://doi.org/10.1016/j.jpowsour.2009.09.059>
- [10] Oetjen, H.-F., Schmidt, V. M., Stimming, U., Trila, F. "Performance data of a proton exchange membrane fuel cell using H₂/Co as fuel gas." *Journal of The Electrochemical Society*. 143, pp. 3838–3842. 1996. <https://doi.org/10.1149/1.1837305>
- [11] Büchi, F. N., Srinivasan, D. "Operating Proton Exchange Membrane Fuel Cells without External Humidification of the Reactant Gases." *Journal of The Electrochemical Society*. 144, pp. 2767–2772. 1997. <https://doi.org/10.1149/1.1837893>
- [12] Uribe, F. A., Gottesfeld, S., Zawodzinski, T. A. "Effect of ammonia as potential fuel impurity on proton exchange membrane fuel cell performance." *Journal of The Electrochemical Society*. 149, pp. A293–A296. 2002. <https://doi.org/10.1149/1.1447221>
- [13] Ticianelli, E. A., Derouin, C. R., Srinivasan, S. "Localization of platinum in low catalyst loading electrodes to attain high power densities in SPE fuel cells." *Journal of Electroanalytical Chemistry and Interfacial Electrochemistry*. 251, pp. 275–295. 1988. [https://doi.org/10.1016/0022-0728\(88\)85190-8](https://doi.org/10.1016/0022-0728(88)85190-8)
- [14] Yao, K. Z., Karan, K., McAuley, K. B., Oosthuizen, P., Peppley, B., Xie, T. "A review of mathematical models for hydrogen and direct methanol polymer electrolyte membrane fuel cells." *Fuel Cells*. 4(1-2), pp. 3–29. 2004. <https://doi.org/10.1002/fuce.200300004>
- [15] Natarajan, D., Nguyen, T. V. "A two-dimensional, two-phase, multi component, transient model for the cathode of a proton exchange membrane fuel cell using conventional gas distributors." *Journal of The Electrochemical Society*. 148(12), pp. A1324–A1335. 2001. <https://doi.org/10.1149/1.1415032>
- [16] Ahmadi, N., Rezazadeh, S., Yekani, M., Fakouri, A., Mirzaee, I. "Numerical investigation of the effect of inlet gases humidity on polymer exchange membrane fuel cell (PEMFC) performance." *Transactions of the Canadian Society for Mechanical Engineering*. 37, pp. 1–20. 2013.
- [17] Lum, K. W., McGuirk, J. J. Three-dimensional model of a complete polymer electrolyte membrane fuel cell – model formulation, validation and parametric studies." *Journal of Power Sources*. 143, pp. 103–124. 2005. <https://doi.org/10.1016/j.jpowsour.2004.11.032>
- [18] Ahmed, D. H., Sung, H. J. "Effects of channel geometrical configuration and shoulder width on PEMFC performance at high current density." *Journal of Power Sources*. 162, pp. 327–339. 2006. <https://doi.org/10.1016/j.jpowsour.2006.06.083>
- [19] Majidifard, S., Mirzaei, I., Rezazadeh, S., Mohajeri, P., Oryani, H. "Effect of Gas Channel Geometry on Performance of PEM Fuel Cells." *Australian Journal of Basic and Applied Sciences*. 5(5), pp. 943–954. 2011.
- [20] Ahmadi, N., Pourmahmoud, N., Mirzaee, I., Rezazadeh, S. "Three-Dimensional Computational Fluid Dynamic Study on performance of polymer exchange membrane fuel cell (PEMFC) in different cell potential." *IJST, Transactions of Mechanical Engineering*. 36(2), pp. 129–141. 2012.
- [21] Ahmadi, N., Pourmahmoud, N., Mirzaee, I., Rezazadeh, S. "Three-Dimensional Computational Fluid Dynamic Study of Effect of Different Channel and Shoulder Geometries on Cell Performance." *Australian Journal of Basic and Applied Sciences*. 5(12), pp. 541–556, 2011.
- [22] Ahmadi, N., Rezazadeh, S., Mirzaee, I., Pourmahmoud, N. "Three-dimensional computational fluid dynamic analysis of the conventional PEM fuel cell and investigation of prominent gas diffusion layers effect." *Journal of Mechanical Science and Technology*. 26(8), pp. 1–11. 2012. <https://doi.org/10.1007/s12206-012-0606-1>
- [23] Ahmed, D. H., Sung, H. J. "Design of a deflected membrane electrode assembly for PEMFCs." *International Journal of Heat and Mass Transfer*. 51, pp. 5443–5453. 2008. <https://doi.org/10.1016/j.ijheatmasstransfer.2007.08.037>
- [24] Wang, L., Husar, A., Zhou, T., Liu, H. "A parametric study of PEM fuel cell performances." *International Journal of Hydrogen Energy*. 28, pp. 1263–1272. 2003. [https://doi.org/10.1016/S0360-3199\(02\)00284-7](https://doi.org/10.1016/S0360-3199(02)00284-7)
- [25] Meredith, R. E., Tobias, C. W. In: *Advances in Electrochemistry and Electrochemical Engineering* 2. Tobias, C. W. (ed.) Interscience Publishers, New York, 1960.